

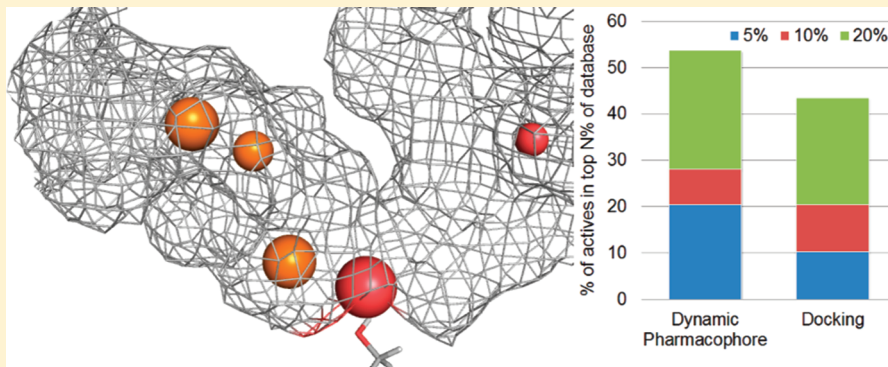
Approximating Protein Flexibility through Dynamic Pharmacophore Models: Application to Fatty Acid Amide Hydrolase (FAAH)

Anna L. Bowman* and Alexandros Makriyannis

Center for Drug Discovery, Northeastern University, Boston, Massachusetts 02115, United States

 Supporting Information

ABSTRACT:



A structure-based drug discovery method is described that incorporates target flexibility through the use of an ensemble of protein conformations. The approach was applied to fatty acid amide hydrolase (FAAH), a key deactivating enzyme in the endocannabinoid system. The resultant dynamic pharmacophore models are rapidly able to identify known FAAH inhibitors over drug-like decoys. Different sources of FAAH conformational ensembles were explored, with both snapshots from molecular dynamics simulations and a group of X-ray structures performing well. Results were compared to those from docking and pharmacophore models generated from a single X-ray structure. Increasing conformational sampling consistently improved the pharmacophore models, emphasizing the importance of incorporating target flexibility in structure-based drug design.

INTRODUCTION

Although it is well known that proteins are inherently flexible, most structure-based drug design methods employ a single, rigid representation of the protein. This approximation has been deemed necessary as the search space for a flexible ligand with a flexible target becomes impractically large. Hence, incorporating protein flexibility without a substantial increase in computational resources remains a challenge.¹ Whereas the functioning of some drug targets is intrinsically linked with their structural flexibility, the substrate- or ligand-binding sites of some seemingly rigid proteins have been shown to be flexible upon small-molecule engagement.² The range of protein conformations arising from this flexibility has a dramatic effect on a ligand's binding pose³ and therefore greatly impacts drug discovery efforts.

Several approaches have been proposed to address the issue of protein flexibility in drug design, including docking methods where permissible rotations of side chains in the binding site are allowed, induced fit docking protocols, and elastic network models.^{1,4,5} Furthermore, multiple techniques utilizing an ensemble of protein conformations, either from experimental sources or molecular dynamics (MD) simulations, have been proposed. These approaches encompass ensemble docking, combining conformers to an average representation, hot-spot mapping over the ensemble, and the relaxed complex method.^{1,4,6}

Here, we present a computational study that focuses on incorporating protein flexibility into structure-based drug discovery as applied to the enzyme, fatty acid amide hydrolase (FAAH). FAAH hydrolytically inactivates various lipid amide signaling molecules including anandamide (AEA), a principal endogenous ligand that engages and activates the G protein-coupled receptors of the endocannabinoid system⁷ and is a system of particular interest in our laboratory.^{8,9} Pharmacological studies have shown that elevated tissue levels of AEA consequent to FAAH inhibition exert substantial therapeutic effects against pain, inflammation, and neuropsychiatric disorders.^{10–13} This indirect mode of activating endocannabinoid system signaling by augmenting local endocannabinoid tone avoids the adverse motor and psychotropic motor side effects associated with systemic application of exogenous cannabinoid receptor-1 agonists.¹⁴ These considerations have made FAAH an attractive therapeutic target for important medical indications, and drug-discovery efforts have led to the discovery of potent FAAH inhibitors with varying mechanisms of action, potencies, and selectivities.^{15–18} FAAH is a membrane-associated protein with an unusual Ser-Ser-Lys catalytic triad. Several X-ray crystallographic structures have provided

Received: August 4, 2011

Published: November 19, 2011

details of the enzyme's binding pockets.^{19–23} FAAH exhibits an arrangement of channels which are involved in substrate orientation and catalysis. The membrane access channel connects the active site to the membrane face of the enzyme, the acyl chain binding channel is thought to accommodate the substrate's acyl chain during catalysis, and the cytosolic port could allow hydrophilic products to exit to the cytosol.²²

We extended a previously reported structure-based pharmacophore model generating approach^{24,25} which utilized a "static" structure (i.e., a single, rigid, conformation of a protein) to a methodology which includes structural variations of the flexible protein. Pharmacophore queries can accommodate target flexibility by altering the radius of the pharmacophore elements and/or excluded volumes.^{26,27} While the use of a static structure can reduce considerably the computational expense of virtual screening or de novo design, it can limit the resulting inhibitors to a small fraction of the appropriate chemical space that could complement the receptor.²⁸ By using multiple protein structures (taken from multiple X-ray crystal structures, NMR ensembles, or generated through MD simulations) to represent an ensemble of conformational states of the receptor, protein flexibility can be incorporated into structure-based drug discovery.^{29–31}

FAAH is a structurally well-characterized enzyme with a diverse set of known inhibitors, making it an optimal test case for the dynamic pharmacophore methodology. This work compares sources of structural ensembles, exploring the influence of different ligands on protein MD snapshots and contrasting the results with those produced from a set of X-ray crystallographic structures. The results for the pharmacophore models are compared to those from traditional docking.

METHODS

Protein Preparation. Rat FAAH (rFAAH) and human FAAH (hFAAH) share high sequence similarity (83% identity and 91% similarity). However, because of difficulties in expressing hFAAH, a large majority of work has been performed with rFAAH. hFAAH and rFAAH have the same catalytic triad (Ser241-Ser217-Lys142), and the active sites are highly conserved with six mutations (Leu192Phe, Phe194Tyr, Ala377Thr, Ser435Asn, Ile491Val, and Val495Met).

X-ray crystallographic structures of rFAAH and humanized rFAAH (in which six active site rFAAH residues were mutated to match those of the human enzyme) were downloaded from the PDB.³² This resulted in nine complexes with unique ligands, PDB IDs 1MT5,¹⁹ 2VY4,²⁰ 2WJ1,²¹ 2WJ2,²¹ 3K7F,²² 3K83,²² 3K84,²² 3LJ6,²³ and 3LJ7.²³ 2WAP has the same ligand as 3LJ6 but at a lower resolution and hence was not used in this study. For each structure of a mutant rFAAH, a homology model was constructed of the wild-type enzyme with prime.³³ The orientation of Asn and Gln side chains and the protonation states for His were optimized and hydrogens minimized to an rmsd limit of 0.3 Å from the starting structure using the Schrödinger protasign and impref utilities, respectively.³⁴

Molecular Dynamics Snapshot Production. Three structures were selected as the starting point for molecular dynamics simulations. The structures were chosen on the basis of the diversity of their complexed ligands: an α -ketooxazole inhibitor (PDB ID 2WJ1); PF3845, a urea-based inhibitor (PDB ID 3LJ6); and URBS97, a carbamate inhibitor (PDB ID 3LJ7) (Figure 1). The backbone of each structure was highly similar. The $C\alpha$ rmsd between 2WJ1 and 3LJ6 is 0.265 Å, between 2WJ1 and 3LJ7 is

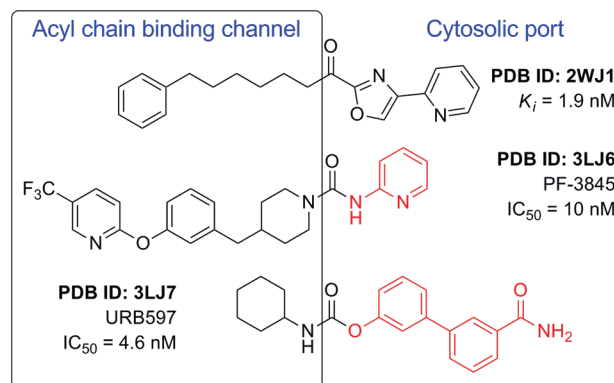


Figure 1. FAAH inhibitors used in MD simulations with orientation in the binding channel indicated. Moieties in red were not present in the X-ray structure.

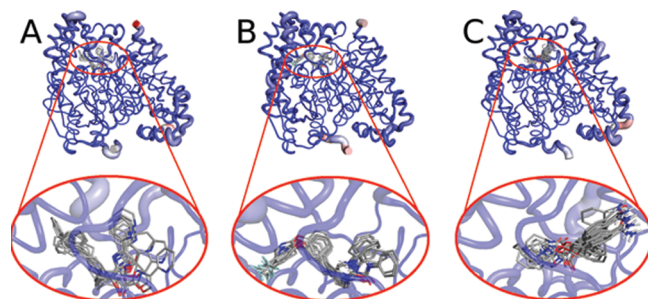


Figure 2. Average backbone structure for MD snapshots from (a) 2WJ1, (b) 3LJ6, and (c) 3LJ7. A red, thicker tube indicates greater rmsd across the ensemble, whereas a blue, narrow tube shows limited flexibility. The oval indicates the substrate-binding site region, and a close up of the region is shown below.

0.266 Å, and between 3LJ6 and 3LJ7 is 0.268 Å. The heavy atom rmsd of active site residues between 2WJ1 and 3LJ6 is 1.311 Å and between 2WJ1 and 3LJ7 1.296 Å; the main difference is the orientation of the Phe432 side chain (2WJ1 Phe432 $\chi_1 = -90^\circ$ and 3LJ6/3LJ7 Phe432 $\chi_1 \approx -173^\circ$). The positions of the active site residues of 3LJ6 and 3LJ7 are more alike, and the heavy atom rmsd is 0.506 Å.

The covalent bond between the catalytic Ser241 and the ligand was broken, and if necessary, any ligand atoms not present in the crystal structure were added in an iterative process based on the position of the available moiety. Each structure was solvated in a box of water extending at least 10 Å from the enzyme. The system was made electrically neutral by replacing six water molecules at the most positive electrostatic potential with six chloride ions. The water and chloride ions were minimized, followed by a full minimization of the entire system. Heavy atoms of the protein complex were held fixed during heating; initially 12 ps were performed in the NVT ensemble at 10 K. This was followed by simulations at 1 atm in the NPT ensemble: 12 ps at 10 K and 24 ps at 300 K. Unrestrained equilibration MD were then performed for 24 ps at 300 K and 1 atm. Finally, unconstrained production MD was performed on each system for 20 ns.

All MD simulations were performed using periodic boundary conditions and a time step of 2 fs. The electrostatic interactions were computed with the particle mesh Ewald (PME) method.^{35,36} The OPLS_2005 all-atom force field and the simple point charge

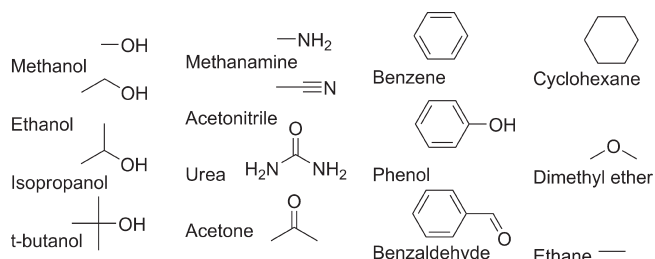


Figure 3. Small-molecule probes used to elucidate binding hot spots in the FAAH binding channels.

(SPC) water model³⁷ were used throughout. All simulations were carried out with the Desmond.^{38,39}

Snapshots were taken every 48 ps during production MD (417 in total) and clustered into 10 bins using the atomic rmsd between backbone atoms with a hierarchical average linkage clustering method (Figure 2). The water molecules, ions, and ligand were removed, and each bin leader was prepared as docking receptors in glide.⁴⁰

Pharmacophore Model Generation. Fifteen probe molecules (Figure 3) were prepared for docking using the LipPrep protocol⁴¹ and the OPLS_2005 force field and docked to each grid at the XP level. Energy terms computed by the Glide XP scoring function are mapped onto the probe atoms.²⁴ The probes are clustered, and energies from each cluster's atoms are summed.²⁵ The clusters are then ranked based on these energies, and the most favorable sites are translated into pharmacophore elements. Optimization of this method found that increasing the ligand diameter midpoint box length from 10 (the default) to 14 Å (the maximum) improved sampling of the binding site.

The pharmacophore models from each MD trajectory were overlaid, and elements which were conserved (present in 50% or more of the ensemble) were retained. The average position of contributing elements determines the center of the each resultant element, with the radius given by the rmsd of contributing elements. In this way protein flexibility is incorporated as only those hot spots which are conserved over a dynamics ensemble are included in the pharmacophore query. A united model was also constructed which utilized the bin leaders from all three trajectories (30 contributing models in total). For comparison, the same protocol was applied to an ensemble of structures comprising of the nine FAAH X-ray structures. Additionally, pharmacophore models based on a single X-ray crystal structure were produced for PDB IDs 2WJ1, 3LJ6, and 3LJ7. The radii for elements of the static pharmacophore models was set at 1.5 Å for aromatic and hydrophobic elements and 1.0 Å for the hydrogen-bond donors and acceptors.²⁵

Excluded volumes were positioned by identifying any atom which is within 3 Å of the ligand in any ensemble. The average position of each atom gives the center of each excluded volume, and the radii are given as 1.5 Å for all atom types.

Creation of the Ligand Database. Thirty nine potent FAAH inhibitors were chosen from the literature with IC₅₀ values in the range 0.047–10 nM.¹⁷ The ligands included representatives from the α -ketone, carbamate, and urea classes along with other miscellaneous FAAH inhibitors (see Supporting Information) and had an average molecular weight of 370. All 39 inhibitors are thought to act by reversible or irreversible covalent modification of the catalytic Ser241. It is likely that in addition to formation of hydrophobic aromatic and hydrogen-bond interactions within

the active site, chemical reactivity contributes to the potency of the compounds. Molecular modeling methods such as docking and pharmacophore models are unable to account for the intrinsic reactivity of an inhibitor. However, these approaches are proficient at identifying ligands that complement the active site, which can help achieve selectivity and improve potency. The FAAH inhibitors were seeded into a database of 1000 decoy ligands with an average molecular weight of 360, taken from the Glide enrichment studies.^{42,43} Multiple conformations of each compound were generated using the conformational import methodology from MOE.⁴⁴

Evaluation of Pharmacophore Models. Each pharmacophore model was screened against the virtual database using MOE.⁴⁴ For models with n pharmacophore elements, screens were performed that required $n - 1$ or $n - 2$ sites to be satisfied, with a minimum of four sites required. However, it should be noted that even if all the crucial pharmacophore elements for FAAH inhibition are present in a single compound other considerations (such as chemical reactivity and stability) also need to be met in order for the compound to be a FAAH inhibitor.⁴⁵ The database was ranked by the lowest rmsd between the pharmacophore models elements and a matching ligand annotation points. To increase the number of hits the radius of each pharmacophore element, given by the rmsd of the contributing elements, was increased by a multiplication factor of 5 for those models derived from MD snapshots and 10 for the model utilizing the X-ray structure ensemble. The results from the pharmacophore model screening were compared to those from docking the same database of 1039 ligands to each of the three MD starting structures at the SP level with Glide.⁴⁰

RESULTS AND DISCUSSION

Performance of Dynamic Pharmacophore Models. Each model was screened against a database of 1000 drug-like decoy molecules seeded with an additional 39 potent FAAH inhibitors. The performance of the pharmacophore models along with those from docking is given in Figure 4. For each MD ensemble, models which required $n - 1$ elements to be satisfied from an n -site model were the most favorable. The most optimal model was that from the 3LJ7 starting structure, with 20.5% of FAAH inhibitors identified in the first 5% of the ranked database and 53.8% of FAAH inhibitors identified in the first 20% of the ranked database. This dynamic pharmacophore model performed better than the docking protocol and the equivalent models from single “static” structures. As well as identifying more actives than the docking protocol, the pharmacophore screening was more rapid than docking, allowing facile searching of much larger databases.²⁷

It is interesting to note the impact that the choice of protein structure, whether for a MD starting structure or to produce a docking grid, has on the predictive nature of the virtual screening. In this case, results using the 2WJ1 coordinates were significantly poorer than those employing the 3LJ7 structure. Such observations are a continuing reminder that a judicious choice should be made when selecting a structure for aiding drug design.⁴⁶

Use of snapshots from all three MD trajectories improved the percentage of FAAH inhibitors identified in the first 5% of the ranked database to 23.1%. Despite the employment of the same snapshots as the single starting structure trajectories, the overall increase in the number of conformations in the ensemble improved the performance of the pharmacophore model.

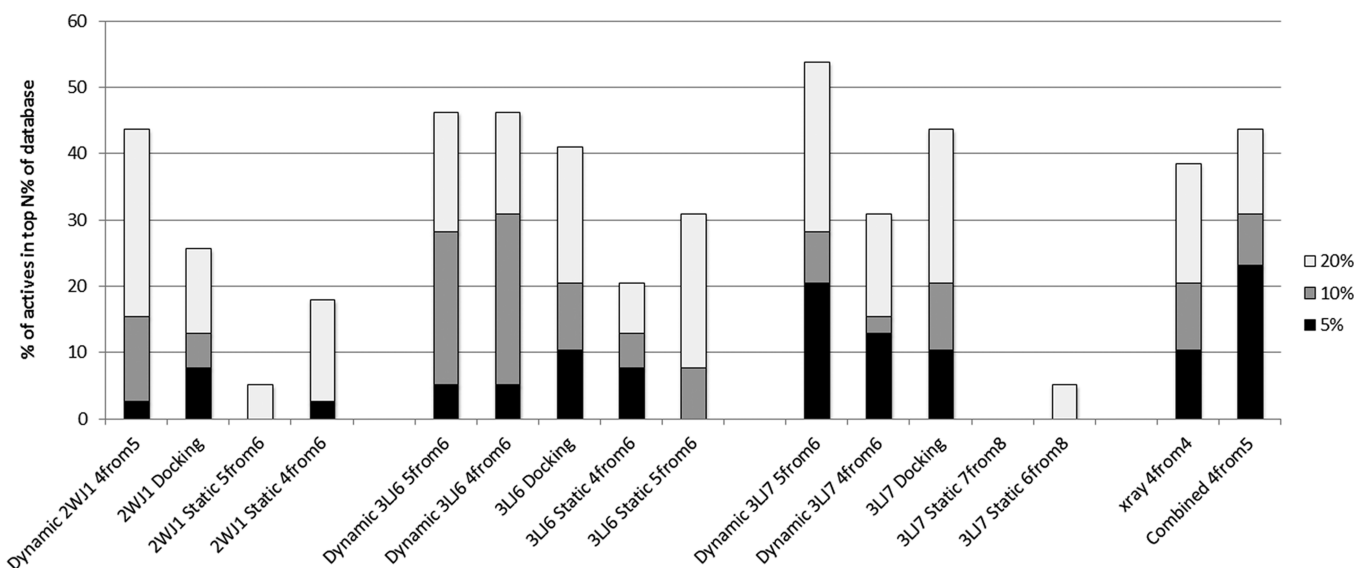


Figure 4. Percentage of actives recovered in the top 5%, 10%, and 20% of the ranked database.

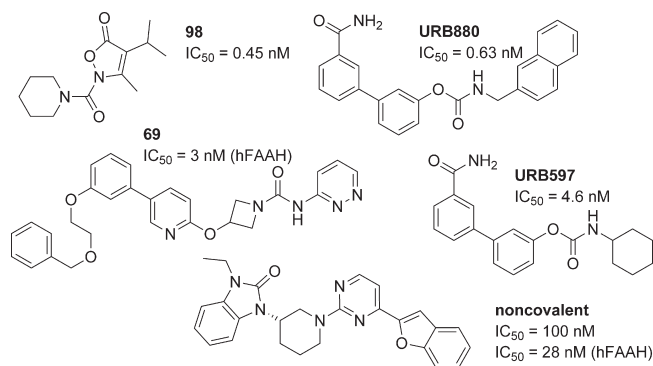


Figure 5. Examples of FAAH inhibitors not highly ranked by dynamic pharmacophore models or docking (98), ranked highly by both methods (URB880), only ranked highly by dynamic pharmacophore models (69), only ranked highly by docking protocols (URBS97), and a noncovalent FAAH inhibitor.

There is some disparity as to the specific FAAH inhibitors being identified by each method, but some parallels are also noted (Figure 5). In general, compounds of low molecular weight with only one or two aromatic centers were not highly ranked by the dynamic pharmacophore models or by the docking protocols, e.g., 98.⁴⁷ It is likely that for inhibitors such as 98, chemical reactivity is a larger contributor to the compounds potency for FAAH than active site complementarity. It is also possible that for such low molecular weight compounds more than one molecule is present in the active site. Compounds with a higher molecular weight and three or four aromatic centers are ranked highly by both methods, e.g., URB880.⁴⁸ A subset of inhibitors was favored by the dynamic pharmacophore models and ranked highly only with this methodology; these compounds featured three or four aromatic centers and could be of larger molecular weight, e.g., 69.⁴⁹ Similarly, several compounds were scored preferentially by the docking protocol; these inhibitors were of lower molecular weight and included two or three aromatic centers, e.g., URB597.⁵⁰

A noncovalent FAAH inhibitor was recently reported⁵¹ and screened separately using the same decoy database of 1000

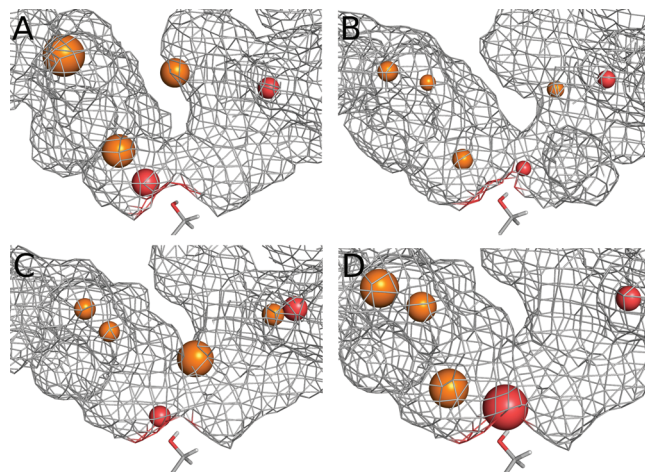


Figure 6. Dynamic pharmacophore models utilizing snapshots from MD trajectories with starting structure taken from PDB ID (a) 2WJ1, (b) 3LJ6, and (c) 3LJ7. (d) United model generated using snapshots from all three trajectories. For clarity, elements of all models are shown with radii of $1 \times \text{rmsd}$ and excluded volumes are not shown. Orange spheres require aromatic interactions, and red spheres are hydrogen-bond acceptors. The catalytic Ser241 is shown in stick representation, and the molecular surface, from 2WJ1, 3LJ6, or 3LJ7 appropriately, is shown in gray (Ser241 and the mesh do not represent any feature of the pharmacophore models).

compounds (Figure 5). Because this compound does not rely on chemical reactivity for potency, it is an excellent test of the dynamic pharmacophore models' ability to identify inhibitors which complement the binding hot spots of FAAH. The noncovalent inhibitor was highly ranked by the dynamic pharmacophore models, having been found in the top 1% of the database screened with the 2WJ1 and 3LJ7 $n - 1$ models, in the top 2% with the 3LJ6 $n - 1$ model, and in the top 3% with the model utilizing all 30 snapshots.

Dynamic Pharmacophore Model Comparison. Each dynamic pharmacophore model consists of two hydrogen-bond

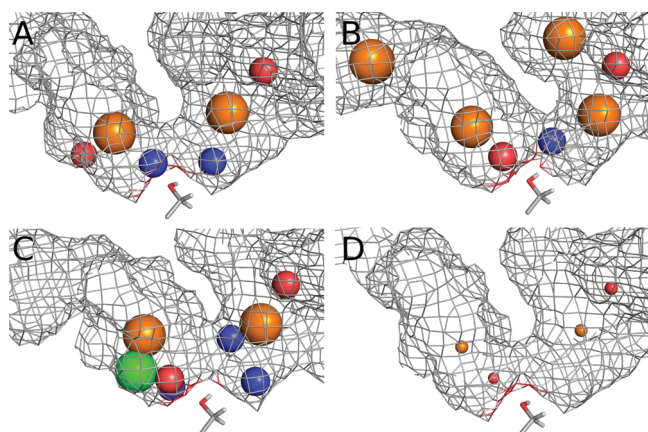


Figure 7. Static pharmacophore models utilizing PDB IDs (a) 2WJ1, (b) 3LJ6, and (c) 3LJ7. (d) Model resulting from an ensemble of nine unique FAAH-inhibitor complexes. For clarity, excluded volumes for all models are not shown and the elements of the X-ray ensemble model are shown with radii of $1 \times \text{rmsd}$. The radii of the aromatic and hydrophobic elements in the static models are 1.5 and 1.0 Å for the hydrogen-bond donors and acceptors. Orange spheres require aromatic interactions, green spheres are hydrophobic, red spheres are hydrogen-bond acceptors, and blue spheres are hydrogen-bond donors. The catalytic Ser241 is shown in stick representation, and the molecular surface, from 2WJ1, 3LJ6, or 3LJ7 appropriately, is shown in gray (Ser241 and the mesh do not represent any feature of the pharmacophore models).

acceptors and either three or four aromatic elements (Figure 6a–c). FAAH–inhibitor interactions can be grouped into three regions: hydrophobic contacts in the acyl-chain binding channel, the catalytic triad and oxyanion hole, and the cytosolic port.

In rFAAH the acyl-chain binding site is a highly hydrophobic region defined by Leu192, Phe194, Phe244, Leu380, Phe381, Leu404, Phe432, Met436, and Ile491. There are two aromatic elements in the acyl-chain binding channel in the 2WJ1 and 3LJ6 dynamic pharmacophore models and three in the 3LJ7 model. These elements reflect the CH–π interactions made between the small-molecule probes and Phe194, Phe381, Phe432, and Met436. The pharmacophore element highest in the acyl-chain binding channel corresponds to the trifluoromethyl pyridine moiety of PF-3845. The neighboring aromatic element, present in the 3LJ6 and 3LJ7 models, corresponds to the *m*-phenylene part of PF-3845.

Every model had a hydrogen-bond acceptor element, reflecting the small-molecule probes interaction with the catalytic Ser241 hydroxyl. The interaction with Ser241 is well known for both reversible and irreversible FAAH inhibitors, and this element corresponds to the crucial carbonyl of many FAAH inhibitors.

The cytosolic port contains one aromatic element in both the 2WJ1 and the 3LJ6 dynamic pharmacophore models and two aromatic elements in the 3LJ7 model. There is also a conserved hydrogen-bond acceptor element in all three models reflecting an interaction with the amine backbone of both Cys269 and Val270. There is crystallographic evidence that certain α-ketoheterocycle-based FAAH inhibitors form hydrogen bonds from the meta substituent on the pyridine ring to both Cys269 NH and Val270 NH (PDB IDs 3K7F and 3K83).^{15,22,52}

United Dynamic Pharmacophore Model Comparison. Five pharmacophore elements were retained when the 10 snapshots from each MD simulation were combined to produce a united model (Figure 6d). There were three aromatic elements in the

acyl-chain binding channel in similar positions to those in the 3LJ6 model. In addition, the two hydrogen-bond acceptor elements seen in the each separate dynamic model are also included. However, no aromatic elements were conserved in the cytosolic port.

Static Pharmacophore Model Comparison. The pharmacophore models derived from a single, static structure performed poorly for this system (Figure 4). Comparison of the models with those from the ensemble of structures reveals some elements in common but also extraneous sites and missing interactions (Figure 7a–c). There is a reduction in the number of aromatic sites in the acyl-chain binding channel. In the model generated from the X-ray structure of PDB ID 2WJ1 an extra hydrogen-bond acceptor is seen in the channel, reflecting the interaction of the small probe molecules with the backbone amine of Phe194. A hydrophobic interaction is seen in the model derived from PDB ID 3LJ7. However, neither of these interactions is conserved over an ensemble of conformations for rFAAH.

The models from PDB IDs 3LJ6 and 3LJ7 both had a hydrogen-bond acceptor element, reflecting the small-molecule probes interaction with the catalytic Ser241 hydroxyl as was seen in the dynamic pharmacophore models. However, there is no analogous element in the model derived from 2WJ1; in its place there is a hydrogen-bond donor element which highlights the probe molecules interaction with the Ser241 hydroxyl oxygen. In the 3LJ7 static pharmacophore model, both a hydrogen-bond donor and hydrogen-bond acceptor describe the interaction with the catalytic serine.

The cytosolic port in each static pharmacophore model contains the highly conserved hydrogen-bond acceptor element seen in the dynamic models (reflecting interactions with the amine backbone of both Cys269 and Val270). An aromatic element is also present, which is conserved among the X-ray structures. In addition, each model contains one or two hydrogen-bond donors reflecting the interaction between the small-molecule probes and Ser217 hydroxyl (2WJ1), Met191 backbone carbonyl (3LJ6 and 3LJ7), and hydroxyl Thr236 (3LJ7). However, none of these interactions are conserved across an ensemble of rFAAH conformations.

X-ray Pharmacophore Model Comparison. The pharmacophore model constructed using the ensemble of X-ray structures did perform highly compared to the static models; however, the performance was similar to that seen in the more successful docking protocols (3LJ6 and 3LJ7) (Figure 4). The model consisted of just four elements (Figure 7d). There are two hydrogen-bond acceptor elements placed in analogous positions to those found in the other rFAAH models, reflecting the small-molecule probes interaction with the catalytic Ser241 hydroxyl and the amine backbone of both Cys269 and Val270. There are also two aromatic elements: one in the acyl-chain binding site and the other in the cytosolic port.

The mean rmsd of heavy atoms in the X-ray structure ensemble to their average structure was 0.48 Å, compared to 1.17, 1.03, and 1.12 Å for analogous rmsd measurement in the 2WJ1, 3LJ6, and 3LJ7 MD ensembles, respectively. Less structural variations in the active site leads to pharmacophore elements with small radii (due to their contributing elements lower RMSDs); this effect is characteristic of models produced from an ensemble of crystal structures.^{30,31} However, despite a close structural similarity among the X-ray structures, the clustering process identified binding hot spots and discarded superfluous elements. The outcome was a model which was much more effective in

identifying FAAH inhibitors over drug-like noninhibitors than models constructed using a single X-ray structure.

Although the ensembles of structures generated from MD simulations yielded a larger range of protein conformations which appears to be advantageous in structure-based drug design, the time involved the running of such simulations may be prohibitive. If an ensemble of X-ray structures is available, its use may provide an expedited route to generating a dynamic pharmacophore model over a MD trajectory without a significant drop in performance.

CONCLUSION

The dynamic pharmacophore method we described here has successfully been able to identify known FAAH inhibitors from a drug-like decoy database. The screening is rapid, and the protocol represents a large improvement over pharmacophore models based on a single static X-ray structure. Dynamic pharmacophore models incorporate protein flexibility and highlight binding hot spots within the protein active site. For FAAH this represents an advantage over docking protocols resulting in more FAAH inhibitors being ranked highly. Increasing conformational sampling by combining snapshots from multiple trajectories resulted in an improved model, emphasizing the importance of incorporating target flexibility.⁵³ Although our prime focus was generating pharmacophore models from MD snapshots, it was shown that utilization of an ensemble of X-ray crystal structures produced similar results without the need for lengthy MD simulations. The main advantage of the dynamic pharmacophore method is that it is a structure-based method independent of known inhibitors; this feature is valuable for targets for which there are a paucity of known ligands and, moreover, can increase the novelty of a hit list.⁵⁴ By highlighting only binding hot spots which are conserved over an ensemble of structures and altering the radius of the resultant pharmacophore elements to reflect the rmsd of the interaction, the method incorporates target flexibility at a much lower cost than docking methods. Additionally, pharmacophore-based screening has an increased throughput when compared to docking methods.

Now that the dynamic pharmacophore method has been shown to be a predictive structure-based approach for FAAH, it can be extended to testing on systems where there are few known inhibitors with hits confirmed through experimental evaluation. It is anticipated that this extension to blind testing will show dynamic pharmacophore models to be an efficient and productive structure-based drug discovery tool.

ASSOCIATED CONTENT

Supporting Information. FAAH inhibitor data set used in this work. This material is available free of charge via the Internet at <http://pubs.acs.org.org>.

AUTHOR INFORMATION

Corresponding Author

*Phone: (617) 373-2273. Fax: (617) 373-7493. E-mail: abowman@neu.edu.

ACKNOWLEDGMENT

This work has been supported by the National Institutes of Health, National Institute on Drug Abuse (grant DA027965).

We thank Dr. Ian Stokes-Rees and SBGrid for maintaining the computers used in this work (National Science Foundation Research Coordination Network, grant 0639193). Part of this work was done using resources provided by the Open Science Grid (supported by the National Science Foundation and the U.S. Department of Energy's Office of Science). We also thank Dr. David Janero for useful discussions.

REFERENCES

- (1) Cozzini, P.; Kellogg, G. E.; Spyros, F.; Abraham, D. J.; Costantino, G.; Emerson, A.; Fanelli, F.; Gohlke, H.; Kuhn, L. A.; Morris, G. M.; Orozco, M.; Pertinez, T. A.; Rizzi, M.; Sottriffer, C. A. Target Flexibility: An Emerging Consideration in Drug Discovery and Design. *J. Med. Chem.* **2008**, *51*, 6237–6255.
- (2) Teague, S. J. Implications of protein flexibility for drug discovery. *Nat. Rev. Drug Discovery* **2003**, *2*, 527–541.
- (3) Erickson, J. A.; Jalaie, M.; Robertson, D. H.; Lewis, R. A.; Vieth, M. Lessons in molecular recognition: The effects of ligand and protein flexibility on molecular docking accuracy. *J. Med. Chem.* **2004**, *47*, 45–55.
- (4) Carlson, H. A. Protein flexibility and drug design: how to hit a moving target. *Curr. Opin. Chem. Biol.* **2002**, *6*, 447–452.
- (5) Sherman, W.; Day, T.; Jacobson, M. P.; Friesner, R. A.; Farid, R. Novel procedure for modeling ligand/receptor induced fit effects. *J. Med. Chem.* **2006**, *49*, 534–553.
- (6) Amaro, R. E.; Baron, R.; McCammon, J. A. An improved relaxed complex scheme for receptor flexibility in computer-aided drug design. *J. Comput. Aided Mol. Des.* **2008**, *22*, 693–705.
- (7) Cravatt, B. F.; Giang, D. K.; Mayfield, S. P.; Boger, D. L.; Lerner, R. A.; Gilula, N. B. Molecular characterization of an enzyme that degrades neuromodulatory fatty-acid amides. *Nature* **1996**, *384*, 83–87.
- (8) Godlewski, G.; Alapafuji, S. O.; Batkai, S.; Nikas, S. P.; Cinar, R.; Offertaler, L.; Osei-Hyiaman, D.; Liu, J.; Mukhopadhyay, B.; Harvey-White, J.; Tam, J.; Pacak, K.; Blankman, J. L.; Cravatt, B. F.; Makriyannis, A.; Kunos, G. Inhibitor of Fatty Acid Amide Hydrolase Normalizes Cardiovascular Function in Hypertension without Adverse Metabolic Effects. *Chem. Biol.* **2010**, *17*, 1256–1266.
- (9) Hwang, J.; Adamson, C.; Butler, D.; Janero, D. R.; Makriyannis, A.; Bahr, B. A. Enhancement of endocannabinoid signaling by fatty acid amide hydrolase inhibition: A neuroprotective therapeutic modality. *Life Sci.* **2010**, *86*, 615–623.
- (10) Cravatt, B. F.; Demarest, K.; Patricelli, M. P.; Bracey, M. H.; Giang, D. K.; Martin, B. R.; Lichtman, A. H. Supersensitivity to anandamide and enhanced endogenous cannabinoid signaling in mice lacking fatty acid amide hydrolase. *Proc. Natl. Acad. Sci. U.S.A.* **2001**, *98*, 9371–9376.
- (11) Ahn, K.; Johnson, D. S.; Mileni, M.; Beidler, D.; Long, J. Z.; McKinney, M. K.; Weerapana, E.; Sadagopan, N.; Liimatta, M.; Smith, S. E.; Lazerwith, S.; Stiff, C.; Kamtekar, S.; Bhattacharya, K.; Zhang, Y. H.; Swaney, S.; Van Beelaere, K.; Stevens, R. C.; Cravatt, B. F. Discovery and Characterization of a Highly Selective FAAH Inhibitor that Reduces Inflammatory Pain. *Chem. Biol.* **2009**, *16*, 411–420.
- (12) Gobbi, G.; Bambico, F. R.; Mangieri, R.; Bortolato, M.; Campolongo, P.; Solinas, M.; Cassano, T.; Morgese, M. G.; Debonnel, G.; Duranti, A.; Tontini, A.; Tarzia, G.; Mor, M.; Trezza, V.; Goldberg, S. R.; Cuomo, V.; Piomelli, D. Antidepressant-like activity and modulation of brain monoaminergic transmission by blockade of anandamide hydrolysis. *Proc. Natl. Acad. Sci. U.S.A.* **2005**, *102*, 18620–18625.
- (13) Cravatt, B. F.; Saghatelyan, A.; Hawkins, E. G.; Clement, A. B.; Bracey, M. H.; Lichtman, A. H. Functional disassociation of the central and peripheral fatty acid amide signaling systems. *Proc. Natl. Acad. Sci. U.S.A.* **2004**, *101*, 10821–10826.
- (14) Jayamanne, A.; Greenwood, R.; Mitchell, V. A.; Aslan, S.; Piomelli, D.; Vaughan, C. W. Actions of the FAAH inhibitor URBS97 in neuropathic and inflammatory chronic pain models. *Br. J. Pharmacol.* **2006**, *147*, 281–288.

- (15) Romero, F. A.; Du, W.; Hwang, I.; Rayl, T. J.; Kimball, F. S.; Leung, D.; Hoover, H. S.; Apodaca, R. L.; Breitenbucher, J. G.; Cravatt, B. F.; Boger, D. L. Potent and selective alpha-ketoheterocycle-based inhibitors of the anandamide and oleamide catabolizing enzyme, fatty acid amide hydrolase. *J. Med. Chem.* **2007**, *50*, 1058–1068.
- (16) Ahn, K.; Johnson, D. S.; Fitzgerald, L. R.; Liimatta, M.; Arendse, A.; Stevenson, T.; Lund, E. T.; Nugent, R. A.; Nomanbhoy, T. K.; Alexander, J. P.; Cravatt, B. F. Novel mechanistic class of fatty acid amide hydrolase inhibitors with remarkable selectivity. *Biochemistry* **2007**, *46*, 13019–13030.
- (17) Deng, H. F. Recent advances in the discovery and evaluation of fatty acid amide hydrolase inhibitors. *Expert Opin. Drug Discovery* **2010**, *5*, 961–993.
- (18) Minkkila, A.; Saario, S. M.; Nevalainen, T. Discovery and Development of Endocannabinoid-Hydrolyzing Enzyme Inhibitors. *Curr. Top. Med. Chem.* **2010**, *10*, 828–858.
- (19) Bracey, M. H.; Hanson, M. A.; Masuda, K. R.; Stevens, R. C.; Cravatt, B. F. Structural adaptations in a membrane enzyme that terminates endocannabinoid signaling. *Science* **2002**, *298*, 1793–1796.
- (20) Mileni, M.; Johnson, D. S.; Wang, Z. G.; Everdeen, D. S.; Liimatta, M.; Pabst, B.; Bhattacharya, K.; Nugent, R. A.; Kamtekar, S.; Cravatt, B. F.; Ahn, K.; Stevens, R. C. Structure-guided inhibitor design for human FAAH by interspecies active site conversion. *Proc. Natl. Acad. Sci. U.S.A.* **2008**, *105*, 12820–12824.
- (21) Mileni, M.; Garfunkle, J.; DeMartino, J. K.; Cravatt, B. F.; Boger, D. L.; Stevens, R. C. Binding and Inactivation Mechanism of a Humanized Fatty Acid Amide Hydrolase by alpha-Ketoheterocycle Inhibitors Revealed from Cocrystal Structures. *J. Am. Chem. Soc.* **2009**, *131*, 10497–10506.
- (22) Mileni, M.; Garfunkle, J.; Ezzili, C.; Kimball, F. S.; Cravatt, B. F.; Stevens, R. C.; Boger, D. L. X-ray Crystallographic Analysis of alpha-Ketoheterocycle Inhibitors Bound to a Humanized Variant of Fatty Acid Amide Hydrolase. *J. Med. Chem.* **2010**, *53*, 230–240.
- (23) Mileni, M.; Kamtekar, S.; Wood, D. C.; Benson, T. E.; Cravatt, B. F.; Stevens, R. C. Crystal Structure of Fatty Acid Amide Hydrolase Bound to the Carbamate Inhibitor URBS97: Discovery of a Deacylating Water Molecule and Insight into Enzyme Inactivation. *J. Mol. Biol.* **2010**, *400*, 743–754.
- (24) Salam, N. K.; Nuti, R.; Sherman, W. Novel Method for Generating Structure-Based Pharmacophores Using Energetic Analysis. *J. Chem. Inf. Model.* **2009**, *49*, 2356–2368.
- (25) Loving, K.; Salam, N. K.; Sherman, W. Energetic analysis of fragment docking and application to structure-based pharmacophore hypothesis generation. *J. Comput. Aided Mol. Des.* **2009**, *23*, 541–554.
- (26) Barillari, C.; Marcou, G.; Rognan, D. Hot-spots-guided receptor-based pharmacophores (HS-Pharm): A knowledge-based approach to identify ligand-anchoring atoms in protein cavities and prioritize structure-based pharmacophores. *J. Chem. Inf. Model.* **2008**, *48*, 1396–1410.
- (27) Sun, H. M. Pharmacophore-based virtual screening. *Curr. Med. Chem.* **2008**, *15*, 1018–1024.
- (28) Carlson, H. A.; McCammon, J. A. Accommodating protein flexibility in computational drug design. *Mol. Pharmacol.* **2000**, *57*, 213–218.
- (29) Bowman, A. L.; Lerner, M. G.; Carlson, H. A. Protein flexibility and species specificity in structure-based drug discovery: Dihydrofolate reductase as a test system. *J. Am. Chem. Soc.* **2007**, *129*, 3634–3640.
- (30) Damm, K. L.; Carlson, H. A. Exploring experimental sources of multiple protein conformations in structure-based drug design. *J. Am. Chem. Soc.* **2007**, *129*, 8225–8235.
- (31) Lerner, M. G.; Bowman, A. L.; Carlson, H. A. Incorporating dynamics in *E. coli* dihydrofolate reductase enhances structure-based drug discovery. *J. Chem. Inf. Model.* **2007**, *47*, 2358–2365.
- (32) Berman, H. M.; Westbrook, J.; Feng, Z.; Gilliland, G.; Bhat, T. N.; Weissig, H.; Shindyalov, I. N.; Bourne, P. E. The Protein Data Bank. *Nucleic Acids Res.* **2000**, *28*, 235–242 <http://www.rcsb.org/pdb/>.
- (33) Prime, version 2.2; Schrödinger, LLC: New York, 2010.
- (34) Impact, version 5.6; Schrödinger, LLC: New York, 2005.
- (35) Darden, T.; York, D.; Pedersen, L. Particle mesh ewald - an N. Log(N) method for Ewald sums in large systems. *J. Chem. Phys.* **1993**, *98*, 10089–10092.
- (36) Essmann, U.; Perera, L.; Berkowitz, M. L.; Darden, T.; Lee, H.; Pedersen, L. G. A smooth particle mesh Ewald method. *J. Chem. Phys.* **1995**, *103*, 8577–8593.
- (37) Berendsen, H. J. C.; Postma, J. P. M.; van Gunsteren, W. F.; Hermans, J. In *Intermolecular Forces*; Pullman, B., Ed.; Reidel: Dordrecht, 1981; pp 331–342.
- (38) Desmond Molecular Dynamics System, version 2.4; D. E. Shaw Research: New York, 2010.
- (39) Maestro-Desmond Interoperability Tools, version 2.4; Schrödinger: New York, 2010.
- (40) Glide, version 5.6; Schrödinger, LLC: New York, 2010.
- (41) LigPrep, version 2.2; Schrödinger, LLC: New York, 2005.
- (42) Friesner, R. A.; Banks, J. L.; Murphy, R. B.; Halgren, T. A.; Klicic, J. J.; Mainz, D. T.; Repasky, M. P.; Knoll, E. H.; Shelley, M.; Perry, J. K.; Shaw, D. E.; Francis, P.; Shenkin, P. S. Glide: A new approach for rapid, accurate docking and scoring. 1. Method and assessment of docking accuracy. *J. Med. Chem.* **2004**, *47*, 1739–1749.
- (43) Halgren, T. A.; Murphy, R. B.; Friesner, R. A.; Beard, H. S.; Frye, L. L.; Pollard, W. T.; Banks, J. L. Glide: A new approach for rapid, accurate docking and scoring. 2. Enrichment factors in database screening. *J. Med. Chem.* **2004**, *47*, 1750–1759.
- (44) Molecular Operating Environment, version 2010.10; Chemical Computing Group Inc.: Montreal, Canada, 2010.
- (45) Vacondio, F.; Silva, C.; Lodola, A.; Fioni, A.; Rivara, S.; Duranti, A.; Tontini, A.; Sanchini, S.; Clapper, J. R.; Piomelli, D.; Mor, M.; Tarzia, G. Structure-Property Relationships of a Class of Carbamate-Based Fatty Acid Amide Hydrolase (FAAH) Inhibitors: Chemical and Biological Stability. *ChemMedChem* **2009**, *4*, 1495–1504.
- (46) Davis, A. M.; St-Gallay, S. A.; Kleywegt, G. J. Limitations and lessons in the use of X-ray structural information in drug design. *Drug Discovery Today* **2008**, *13*, 831–841.
- (47) Minkkila, A.; Savinainen, J. R.; Kasnanen, H.; Xhaard, H.; Nevalainen, T.; Laitinen, J. T.; Poso, A.; Leppanen, J.; Saario, S. M. Screening of Various Hormone-Sensitive Lipase Inhibitors as Endocannabinoid-Hydrolyzing Enzyme Inhibitors. *ChemMedChem* **2009**, *4*, 1253–1259.
- (48) Mor, M.; Lodola, A.; Rivara, S.; Vacondio, F.; Duranti, A.; Tontini, A.; Sanchini, S.; Piersanti, G.; Clapper, J. R.; King, A. R.; Tarzia, G.; Piomelli, D. Synthesis and quantitative structure-activity relationship of fatty acid amide hydrolase inhibitors: Modulation at the N-portion of biphenyl-3-yl alkylcarbamates. *J. Med. Chem.* **2008**, *51*, 3487–3498.
- (49) Roughley, S.; Walls, S.; Hart, T.; Parsons, R.; Brough, P.; Graham, C.; Macias, A. Azetidine derivatives as inhibitors of fatty acid amide hydrolase useful in the treatment of diseases and preparation and pharmaceutical compositions thereof. WO2009109743, 2009.
- (50) Mor, M.; Rivara, S.; Lodola, A.; Plazzi, P. V.; Tarzia, G.; Duranti, A.; Tontini, A.; Piersanti, G.; Kathuria, S.; Piomelli, D. Cyclohexylcarbamic acid 3'- or 4'-substituted biphenyl-3-yl esters as fatty acid amide hydrolase inhibitors: Synthesis, quantitative structure-activity relationships, and molecular modeling studies. *J. Med. Chem.* **2004**, *47*, 4998–5008.
- (51) Min, X. S.; Thibault, S. T.; Porter, A. C.; Gustin, D. J.; Carlson, T. J.; Xu, H. D.; Lindstrom, M.; Xu, G. F.; Uyeda, C.; Ma, Z. H.; Li, Y. H.; Kayser, F.; Walker, N. P. C.; Wang, Z. L. Discovery and molecular basis of potent noncovalent inhibitors of fatty acid amide hydrolase (FAAH). *Proc. Natl. Acad. Sci. U.S.A.* **2011**, *108*, 7379–7384.
- (52) Kimball, F. S.; Romero, F. A.; Ezzili, C.; Garfunkle, J.; Rayl, T. J.; Hochstatter, D. G.; Hwang, I.; Boger, D. L. Optimization of alpha-ketooxazole inhibitors of fatty acid amide hydrolase. *J. Med. Chem.* **2008**, *51*, 937–947.
- (53) Lexa, K. W.; Carlson, H. A. Full protein flexibility is essential for proper hot-spot mapping. *J. Am. Chem. Soc.* **2011**, *133*, 200–202.
- (54) Carlson, H. A. Protein flexibility is an important component of structure-based drug discovery. *Curr. Pharm. Design* **2002**, *8*, 1571–1578.